



HAL
open science

A global OCIO stratospheric layer discovered in GOMOS stellar occultation measurements

Didier Fussen, Filip Vanhellemont, Jan Dodion, Christine Bingen, Nina Mateshvili, Frank Daerden, Dominique Fonteyn, Quentin Errera, Simon Chabrillat, Erkki Kyrölä, et al.

► To cite this version:

Didier Fussen, Filip Vanhellemont, Jan Dodion, Christine Bingen, Nina Mateshvili, et al.. A global OCIO stratospheric layer discovered in GOMOS stellar occultation measurements. *Geophysical Research Letters*, 2006, 33 (13), pp.L13815. 10.1029/2006GL026406 . hal-00086125

HAL Id: hal-00086125

<https://hal.science/hal-00086125>

Submitted on 13 Jul 2017

HAL is a multi-disciplinary open access archive for the deposit and dissemination of scientific research documents, whether they are published or not. The documents may come from teaching and research institutions in France or abroad, or from public or private research centers.

L'archive ouverte pluridisciplinaire **HAL**, est destinée au dépôt et à la diffusion de documents scientifiques de niveau recherche, publiés ou non, émanant des établissements d'enseignement et de recherche français ou étrangers, des laboratoires publics ou privés.

A global OCIO stratospheric layer discovered in GOMOS stellar occultation measurements

Didier Fussen,¹ Filip Vanhellemont,¹ Jan Dodion,¹ Christine Bingen,¹ Nina Matshvili,¹ Frank Daerden,¹ Dominique Fonteyn,¹ Quentin Errera,¹ Simon Chabrillat,¹ Erkki Kyrölä,² Johanna Tamminen,² Viktoria Sofieva,² Alain Hauchecorne,³ Francis Dalaudier,³ Jean-Loup Bertaux,³ Jean-Baptiste Renard,⁴ Renaud Fraisse,⁵ Odile Fanton d'Andon,⁶ Gilbert Barrot,⁶ Marielle Guirlet,⁶ Antoine Mangin,⁶ Thorsten Fehr,⁷ Paul Snoeij,⁷ and Lidia Saavedra⁷

Received 24 March 2006; revised 3 May 2006; accepted 6 June 2006; published 15 July 2006.

[1] The stratospheric ozone depletion observed in polar regions is caused by several catalytic cycles induced by reactive chlorine and bromine species. By reacting with BrO, ClO causes the formation of OCIO which is considered as a proxy of the halogen activation. We present the first global determination of the stratospheric OCIO distribution measured during the year 2003 by the stellar occultation spectrometer GOMOS. Besides its expected polar abundance, we discovered the presence of a worldwide OCIO layer in the upper stratosphere. At lower altitudes, OCIO seems also to be present beyond the limit of the polar vortices, an unreported feature. **Citation:** Fussen, D., et al. (2006), A global OCIO stratospheric layer discovered in GOMOS stellar occultation measurements, *Geophys. Res. Lett.*, 33, L13815, doi:10.1029/2006GL026406.

[2] The quantitative explanation of the recurrent polar ozone hole during springtime requires an accurate knowledge of the ClO and BrO number density vertical profiles. Important progress has been made in the last decade to improve our understanding of the inorganic chlorine (Cl_y) chemistry. Chlorine reservoir gases (such as ClONO₂ and HCl) are converted into reactive species (ClO and ClOOCl) at the surface of particles present in polar stratospheric clouds. These species are responsible for a very efficient catalytic destruction of ozone if they are not inactivated by a conversion into reservoir gases such as HCl or ClONO₂, a process that is weakened by the polar denitrification in the presence of polar stratospheric clouds. A direct consequence of the halogen activation is the production of OCIO via the main branch of the reaction (1a) (see the 2002 JPL kinetics report by Sander et al. [2003]) involving both ClO and BrO:



[3] Although OCIO is not directly responsible for the ozone destruction, it plays a fundamental role in the Cl_y budget and the correct modelling of its abundance is a crucial test for our understanding of the stratospheric halogen chemistry. The major sink for OCIO is its rapid photolysis by the solar radiation due to a large absorption cross section well characterized by a strong differential structure in the UV wavelength range. This feature has allowed the measurement of OCIO, a species that is only present at very small concentrations.

[4] Since the first detection of atmospheric OCIO in Antarctica [Solomon et al., 1987], total column densities were retrieved from ground-based, airborne and satellite measurements, however mostly above polar regions because the halogen activation is expected to occur there [Wagner et al., 2001] and also due to the limitations imposed by the use of the limb scattering technique [Krecl et al., 2005]. So far, the measurement of the vertical profile of the OCIO number density has been performed in a very limited number of experiments and only in polar regions. The determination of the OCIO vertical concentration during night time turned out to be an even more difficult measurement and can only be performed by using lunar or stellar radiation. Very few results have been reported [Krecl et al., 2005; Pommereau and Piquard, 1994; Renard et al., 1997; Rivière et al., 2002], again only in polar regions.

[5] GOMOS (Global Ozone Monitoring by Occultation of Stars) on the European ENVISAT satellite is the first space instrument dedicated to the atmospheric remote sounding of the Earth by using the stellar occultation method [Kyrölä, 2004]. From a heliosynchronous orbit, it almost covers the full latitude range and the instrument self-calibration is particularly well adapted to the long time trend monitoring of stratospheric species. The wavelength coverage of 245 nm to 942 nm allows the monitoring of ozone, H₂O, NO₂, NO₃, air, aerosols, O₂ and the temperature profiles. Although it was one of the target species to be retrieved in the original GOMOS proposal, the small OCIO slant path optical thickness with respect to the instrumental signal-to-noise (SNR) ratio makes it almost impossible to

¹Institut d'Aéronomie Spatiale de Belgique, Bruxelles, Belgium.

²Finnish Meteorological Institute, Helsinki, Finland.

³Service d'Aéronomie du CNRS, Verrières-le-Buisson, France.

⁴Laboratoire de Physique et Chimie de l'Environnement, Orléans, France.

⁵Astrium, Toulouse, France.

⁶ACRI-ST, Sophia-Antipolis, France.

⁷European Space Research Institute (ESRIN), European Space Agency, Frascati, Italy.

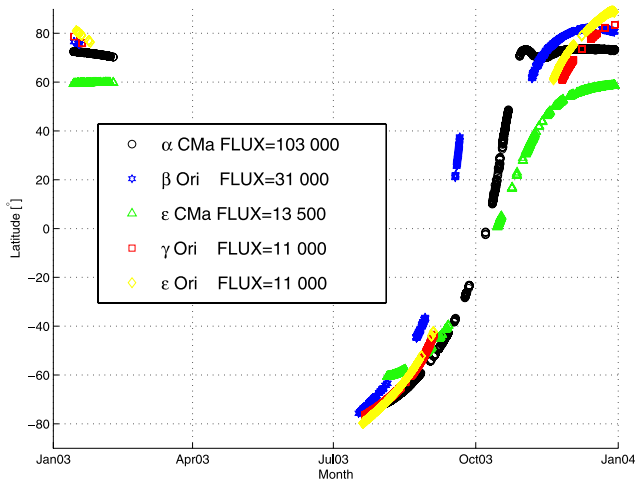


Figure 1. GOMOS dark limb measurements during the year 2003: geolocation of the occultation tangent points for the 5 brightest stars available in the selected OCIO spectral window (Flux number is expressed in arbitrary units).

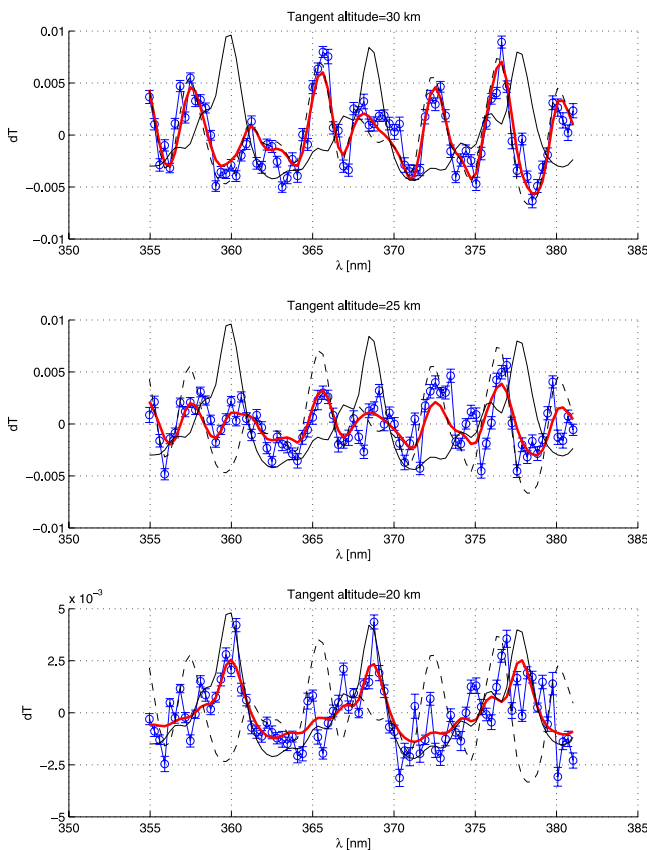


Figure 2. The GOMOS averaged differential transmittance at 3 different tangent altitudes: 30, 25, and 20 km from top to bottom. Blue circles/thin blue line: experimental data with error bars. Full red line: best DOAS fit obtained. The thin full and dashed black lines respectively refer to the OCIO and NO_2 differential cross sections (arbitrary units).

retrieve in the processing of individual occultations. Instead, we have increased the SNR by co-adding weighted transmittances (reduced to a common tangent altitude grid) in latitude bins of 5 degrees with a typical time resolution of about one month. In Figure 1, the geolocation sites of about 4500 occultations used in the binning have been reported for the year 2003. It is important to realize that the global results presented here switch progressively from the southern polar winter (July) to the northern polar hemisphere (Dec–Jan). This constraint was imposed by the astronomical availability of the five most emitting stars in the useful OCIO absorption range [355–390 nm].

[6] The retrieval of the OCIO slant path column density has been performed by using a differential optical absorption spectroscopy (DOAS) approach applied to the experimental differential transmittance $dT(\lambda)$, the difference between the measured transmittance $T(\lambda)$ and the smoothed

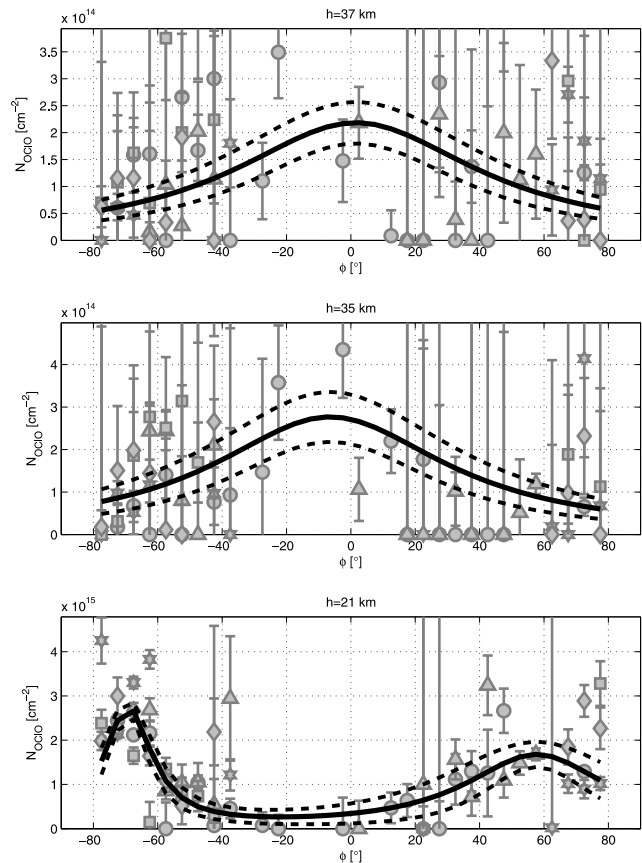


Figure 3. The OCIO slant column densities retrieved independently for the 5 stars (with the same symbols as in Figure 1) with the spectral inversion error bars. The full line is the result of an error-weighted fit by the sum of two Lorentzian distributions with the associated confidence interval at the 1- σ level. (top) Tangent altitude equals 37 km. (middle) Tangent altitude equals 35 km. (bottom) Tangent altitude equals 21 km. The reported values cover a time period of about 6 months (see Figure 1). Notice the clear change in the latitudinal distribution between the lower and the upper equatorial stratosphere.

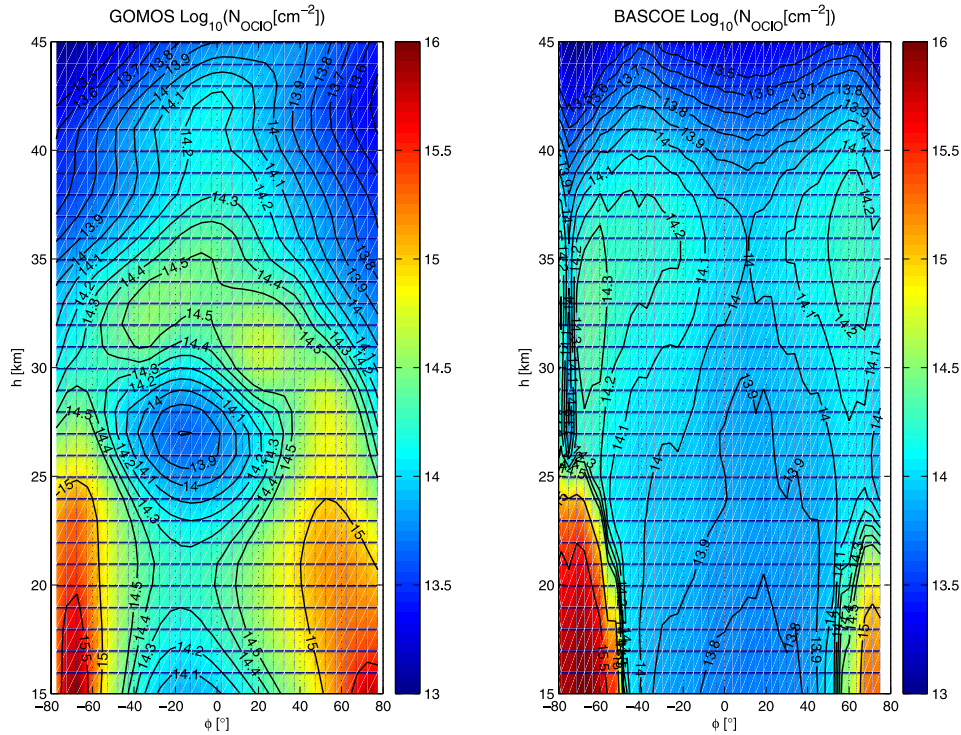


Figure 4. Isopleths (latitude-altitude) of the OCIO slant column densities measured by GOMOS and modelled by the BASCOE model at the same geolocation and time for the measurement periods [Jan 14–Feb 9, 2003] and [Jul 20–Dec 30, 2003] as reported in Figure 1.

transmittance $T_s(\lambda)$. The modelled differential transmittance $M(\lambda)$ is written as:

$$M(\lambda) = T_s(\lambda) \left(1 - \exp \left(- [N_{O_3} \delta\sigma_{O_3} + N_{NO_2} \delta\sigma_{NO_2} + N_{OCIO} \delta\sigma_{OCIO}] \right) \right) \quad (2)$$

where N_i are the slant columns and $\delta\sigma_i(\lambda + \Delta\lambda)$ the respective differential cross sections possibly shifted by $\Delta\lambda$. In order to avoid difficulties with the behaviour of the statistical distribution of measured values for very small optical thicknesses, equation (2) is not linearized. Instead, the N_{OCIO} is obtained by a nonlinear least-squares minimization of the difference between $M(\lambda)$ and $dT(\lambda)$ weighted by the experimental errors and the retrieval random error is extracted from the Jacobian. This spectral inversion algorithm was applied independently for each tangent altitude (1 km step) between 15 and 45 km and also independently for each of the 5 selected stars in order to check the consistency of the retrieval for stars having different magnitudes, temperatures and setting angles. In Figure 2 we show the averaged transmittances obtained from 64 Sirius (α_{CMa} , Magnitude = -1.44 , Temperature = 11 000 K) occultations observed between $75^\circ S$ and $70^\circ S$ (about 1 week around Aug 1, 2003). The differential transmittance at a tangent altitude of 30 km is dominated by NO_2 absorption features whereas the OCIO signature is clearly observed at 20 km.

[7] In Figure 3, we present the latitudinal variation of the measured OCIO slant column densities obtained for three tangent altitudes: at 21 km, two well defined maxima (2.5×10^{15} and 1.5×10^{15} cm^{-2}) are visible in the “activated”

polar regions that were however sampled with a 6-month time interval. It is interesting to notice the presence of OCIO outside the polar vortex and this is particularly striking at mid-latitudes in the northern hemisphere. In the upper stratosphere ($h = 35$ km, 37 km), another picture emerges. The latitudinal OCIO distribution has a bell-shaped form centred on equatorial regions and a clear positive gradient exists from the poles toward the equator. Despite the large error bars associated with some latitude bins, there is a reasonable agreement between the results obtained from different stars. In Figure 4, we show the isopleths of the full latitude-altitude OCIO slant column distribution. One may also notice the progressive change in the OCIO upper stratospheric layer until it vanishes in the polar regions.

[8] Although the presence of a global OCIO layer in the upper stratosphere has not been reported so far due to the lack of instruments capable of performing nighttime measurements, we have compared our data with the results of the BASCOE model [Errera and Fonteyn, 2001], a 3-D chemical transport code driven by assimilated ECMWF wind fields and evaluated at the same spatio-temporal locations of the GOMOS measurements. Within a factor 2, the presence of OCIO at about 35 km is well confirmed by the model on a global scale with some enhancement toward the polar regions, a feature not observed by GOMOS. However, CIO (and subsequently OCIO) may have been strongly depleted by a strong polar enhancement of NO_2 observed after the Oct–Nov 2003 exceptional solar proton event [Seppälä et al., 2004] which is not simulated by the model. A second qualitative difference in the GOMOS data is the larger

latitudinal extension (well outside the vortex regions) of OCIO in the northern hemisphere.

[9] The inspection of the modelled OCIO source and sink terms revealed that reaction (1) is univocally responsible for OCIO production in the stratosphere. Such dependence should therefore be reflected by the vertical concentration profiles of ClO and BrO, for which lifetimes considerably increase above 35 km when they are less depopulated by the 3-body reaction with NO₂ [Dessler, 2000]. The MLS measurements (see Waters et al., electronic material, 2005, available at <http://mls.jpl.nasa.gov/>) of ClO clearly show a maximum at about 40 km. This results from the strong diurnal cycle affecting all these constituents through the NO₂ photolysis in the daylight but also from the lower pressure. Consequently, ClO and BrO are much more efficiently destroyed during the night at 25 km than in the upper stratosphere leading to the enhancement of the OCIO in that region. Also, the OCIO production will depend on the available reaction partners at sunset and the large BrO daytime abundance predicted by BASCOE around 20 km could be the cause for the presence of OCIO in the lower stratosphere outside of the polar vortices.

[10] Future work will make use of the forthcoming complete processing of GOMOS data for the period 2002–2005 and will also address seasonal and annual variations. Apart from its confirmed role of being a proxy for stratospheric ClO and BrO, the OCIO global measurement is a crucial test to quantitatively assess the relative impact of the background chemistry involving halogen compounds on the occurrence of the polar ozone hole.

[11] **Acknowledgment.** This work has been partly supported by the PRODEX 8 project “SADE” and by the research project MO/35/009 under the authority of the Belgian Federal Science Policy Office.

References

- Dessler, A., (2000), *The Chemistry and Physics of Stratospheric Ozone*, Elsevier, New York.
- Errera, Q., and D. Fonteyn (2001), Four-dimensional variational chemical assimilation of CRISTA stratospheric measurements, *J. Geophys. Res.*, *106*, 12,253–12,266.
- Krecl, P., C. S. Haley, J. Stegman, S. M. Brohede, and G. Berthet (2005), Retrieving the vertical distribution of stratospheric OCIO from Odin/OSIRIS limb-scattered sunlight measurements, *Atmos. Chem. Phys. Disc.*, *5*, 2989–3045.
- Kyrölä, E. (2004), GOMOS on Envisat: An overview, *Adv. Space Res.*, *33*, 1020–1028.
- Pommereau, J. P., and J. Piquard (1994), Observations of the vertical distribution of stratospheric OCIO, *Geophys. Res. Lett.*, *21*, 1231–1234.
- Renard, J.-B., F. Lefèvre, M. Pirre, C. Robert, and D. Hugué (1997), Vertical profile of night-time stratospheric OCIO, *J. Atmos. Chem.*, *26*, 65–76.
- Rivière, E. D., M. Pirre, G. Berthet, J.-B. Renard, F. G. Taupin, N. Huret, M. Chartier, B. Knudsen, and F. Lefèvre (2002), On the interaction between nitrogen and halogen species in the Arctic polar vortex during THESEO and THESEO 2000, *J. Geophys. Res.*, *108*(D5), 8311, doi:10.1029/2002JD002087.
- Sander, S. P., et al. (2003), Chemical kinetics and photochemical data for use in atmospheric studies, *JPL Publ. 02–25*, Jet Propul. Lab., Pasadena, Calif.
- Seppälä, A., P. T. Verronen, E. Kyrölä, S. Hassinen, L. Backman, A. Hauchecorne, J. L. Bertaux, and D. Fussen (2004), Solar proton events of October–November 2003: Ozone depletion in the Northern Hemisphere polar winter as seen by GOMOS/Envisat, *Geophys. Res. Lett.*, *31*, L19107, doi:10.1029/2004GL021042.
- Solomon, S., G. H. Mount, R. W. Sanders, and A. L. Schmeltekopf (1987), Visible spectroscopy at McMurdo Station, Antarctica 2. Observations of OCIO, *J. Geophys. Res.*, *92*, 8329–8338.
- Wagner, T., C. Leue, K. Pfeilsticker, and U. Platt (2001), Monitoring of the stratospheric chlorine activation by Global Ozone Monitoring Experiment (GOME) OCIO measurements in the austral and boreal winters 1995 through 1999, *J. Geophys. Res.*, *106*, 4971–4986.
- J.-L. Bertaux, F. Dalaudier, and A. Hauchecorne, Service d’Aéronomie du CNRS, BP 3, F-91371 Verrières-le-Buisson, France.
- C. Bingen, S. Chabrilat, F. Daerden, J. Dodion, Q. Errera, D. Fonteyn, D. Fussen, N. Mateshvili, and F. Vanhellemont, Institut d’Aéronomie Spatiale de Belgique, 3, avenue Circulaire, B-1180, Bruxelles, Belgium. (didier.fussen@oma.be)
- O. F. d’Andon, G. Barrot, M. Guirlet, and A. Mangin, ACRI-ST, 260, route du Pin Montard, BP 234, F-06904 Sophia-Antipolis, France.
- T. Fehr, L. Saavedra, and P. Snoeij, European Space Research Institute (ESRIN), European Space Agency, Via Galileo Galilei, I-00044 Frascati, Italy.
- R. Fraise, Astrium, 31, avenue des Cosmonautes, F-31402 Toulouse cedex 4, France.
- E. Kyrölä, V. Sofieva, and J. Tamminen, Finnish Meteorological Institute, P.O. Box 503, FIN-001010 Helsinki, Finland.
- J.-B. Renard, Laboratoire de Physique et Chimie de l’Environnement, A, avenue de la Recherche Scientifique, F-45071, Orléans cedex 2, France.